ISSN: 1410-8917
Jurnal Kimia Sains & Aplikasi
e-ISSN: 2597-9914

Jurnal Kimia Sains dan Aplikasi 29 (4) (2026): 265-275

Jurnal Kimia Sains dan Aplikasi
Journal of Scientific and Applied Chemistry

Journal homepage: http://ejournal.undip.ac.id/index.php/ksa

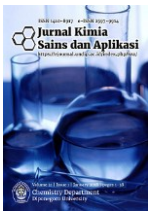

Optimization of Chitin Extraction and Conversion to Chitosan from Black Soldier Fly (*Hermetia illucens*) Pupae for Sustainable Biopolymer Production

Purwantiningsih Sugita [1], Muhammad Qurthubi Ash Shiddiqi [2], Kurniawanti [1], Dewi Apri Astuti [3,*]

[1] Department of Chemistry, Faculty of Mathematics and Natural Sciences, IPB University, Bogor, West Java, Indonesia
[2] Undergraduate Chemistry student, Department of Chemistry, Faculty of Mathematics and Natural Sciences, IPB University, Bogor, West Java, Indonesia
[3] Department of Nutrition and Feed Technology, Faculty of Animal Science, IPB University, Bogor 16680, Indonesia

* Corresponding author: dewiaa@apps.ipb.ac.id

https://doi.org/10.14710/jksa.29.4.265-275

Article Info

Article history:

Received: 24th December 2025
Revised: 31st March 2026
Accepted: 31st March 2026
Online: 25th May 2026

Keywords:
Black soldier fly; Box-Behnken design; chitin; chitosan; process optimization

Abstract

Chitin and its derivative, chitosan, are natural polysaccharides with wide industrial applications due to their biodegradability and multifunctional biological activities. The black soldier fly (*Hermetia illucens*, BSF) represents a promising alternative source of chitin beyond conventional crustacean shells. However, studies on the optimization of chitin isolation from BSF pupae exuviae remain limited. This study aims to optimize the demineralization and deproteinization stages of chitin isolation and conversion to chitosan using a Box–Behnken design in Design-Expert 13. The effects of acid/base concentration, immersion time, and temperature were statistically evaluated to maximize chitin yield. The optimized conditions (3 M HCl, 1 M NaOH, 25°C, 1 h) resulted in a predicted chitin yield of 52.12%, which was experimentally validated to produce 50.83%. The isolated chitin had a low ash content (1.21%), indicating effective mineral removal and confirming its relatively high purity. The isolated chitin was subsequently deacetylated to chitosan, yielding 36% product with a degree of deacetylation (DD) of 53%. FTIR and XRD analyses confirmed the formation of partially deacetylated chitosan with a crystallinity index of 57%. It is concluded that the Box–Behnken optimization effectively enhanced process efficiency and enabled the systematic identification of optimal extraction conditions from BSF pupae shells, demonstrating their strong potential as a sustainable, non-crustacean source of chitin and chitosan for future biopolymer and green-material applications.

1. Introduction

Chitin, a β-(1,4)-N-acetyl-D-glucosamine polymer, is the second most abundant natural polysaccharide after cellulose and serves as a structural component in the exoskeletons of arthropods, fungi, and mollusks [1]. Its deacetylated derivative, chitosan, is a biopolymer with excellent biodegradability, biocompatibility, and bioactivity, enabling a wide range of applications in food, pharmaceuticals, agriculture, and wastewater treatment [2, 3, 4]. Commercially, chitin is primarily obtained from the shells of shrimp and crabs [5]. However, the dependence on marine crustaceans presents sustainability and allergenicity concerns, motivating the search for alternative sources such as squid, cuttlefish, lobster, crayfish, spiders, and insects, including beetles and silkworms [6, 7].

Insects have recently emerged as a renewable and underexploited source of chitin. Among them, the black soldier fly (*Hermetia illucens*, BSF) has attracted increasing attention due to its rapid growth, high protein and lipid content, and ability to convert organic waste into valuable biomass [8, 9, 10]. The exoskeleton of BSF

contains substantial amounts of chitin (20–35%) that can be isolated from pupae shells, a major by-product of larval cultivation [11]. Compared to crustacean chitin, BSF-derived chitin exhibits crystallinity values that vary widely depending on developmental stage and extraction conditions (25–35%), which enhances its chemical reactivity and adsorption capacity due to increased amorphous regions, making it suitable for biosorption and material modification applications [12].

Despite increasing research on insect chitin, most studies on BSF have focused on direct extraction using single-factor experiments without systematic optimization. Critical process parameters such as acid/base concentration, temperature, and extraction duration significantly affect yield and chitin quality [13, 14]. The absence of statistically optimized protocols limits understanding of the process and its optimization potential. The findings are expected to enhance understanding and optimization of processes and promote the use of insect biomass for chitin production at an industrial scale.

To address this gap, the present study applies a Response Surface Methodology (RSM) with Box–Behnken design to optimize the demineralization and deproteinization stages during chitin isolation from BSF pupae shells. This statistical approach allows the evaluation of interactive effects among multiple variables and the determination of optimal conditions that maximize chitin yield. This study provides the first Box–Behnken optimization of BSF chitin extraction reported in Indonesia, integrating statistical design with chemical characterization to improve process optimization and efficiency. The optimized chitin was subsequently converted to chitosan and characterized using FTIR and XRD to evaluate its structural transformation and crystallinity. The findings contribute to the valorization of insect biomass as a sustainable source of industrial-grade biopolymers, supporting circular bioeconomy initiatives and waste-to-resource strategies.

2. Experimental

2.1. Materials

Pupal exuviae of the black soldier fly (*Hermetia illucens*) were obtained from a local BSF cultivation by using organic waste substrates from the Department of Nutrition and Feed Technology, Faculty of Animal Science, IPB University, Bogor, Indonesia. The samples were thoroughly washed with distilled water to remove adhering impurities, dried in the sunlight, ground in a blender, and sieved to obtain uniform particles (<500 µm). Analytical grade reagents, including hydrochloric acid (HCl), sodium hydroxide (NaOH), and sodium hypochlorite (NaOCl), were purchased from Merck (Germany). All solutions were prepared using distilled water.

2.2. Experimental Design for Process Optimization

The optimisation of the demineralisation (HCl treatment) and deproteinisation (NaOH treatment) stages was performed using Response Surface Methodology (RSM) based on a Box–Behnken Design (BBD) in Design-Expert version 13 (Stat-Ease Inc., USA). Six factors were selected as independent variables: HCl concentration, time, and temperature for demineralisation, and NaOH concentration, time, and temperature for deproteinization. The solid-to-liquid ratio was fixed at 1:20 (w/v). The experimental design and optimisation model are shown in Table 1. The design produced 51 experimental runs, including centre points to estimate experimental error and assess model robustness. The response variable was the chitin yield (%). All experiments were performed in duplicate, and the average values were used for statistical modelling.

2.3. Isolation of Chitin

Ground BSF pupae powder (10 g) was subjected to acid treatment for demineralisation using HCl solutions (1–3 M) at varying temperatures (25–50°C) and immersion times (1–3 h) according to the conditions listed in Table 1. The solid-to-liquid ratio was maintained at 1:20 (w/v). Demineralisation using HCl was performed to remove inorganic minerals, particularly calcium carbonate, from the pupal shell matrix [15]. Following demineralisation, the residue was filtered, thoroughly rinsed with distilled water to neutrality, and then subjected to deproteinization using NaOH solutions (1 – 3 M) under the same ratio (1:20 w/v) with varying temperature and time (25–50°C; 1–3 h).

Deproteinization is a key step designed to remove proteinaceous materials, which can be achieved through either chemical or biological means [16]. Chemically, this process typically employs strong bases such as NaOH or KOH [17]. The filtrates obtained from both demineralisation and deproteinization were subsequently analysed for metal and amino acid contents, respectively. Metal content was determined using ICP-OES (Agilent Technologies 5100) after acid digestion of the samples with nitric acid. Calibration was carried out using certified standard solutions [18]. Amino acid composition was analysed using HPLC (Shimadzu SCL-10A) after hydrolysis with 6 M HCl at 110°C for 24 h [19].

Table 1. Experimental design and optimization model

Factor	Parameter	Unit	Range	Type
Demineralization	HCl concentration	M	1–3	Numerical
	Maceration Time	h	1–3	Numerical
	Temperature	°C	25–50	Numerical
Deproteinization	NaOH concentration	M	1–3	Numerical
	Maceration Time	h	1–3	Numerical
	Temperature	°C	25–50	Numerical

A depigmentation step was then conducted by immersing the chitin in 12% NaOCl under continuous stirring for 10 mins. This step eliminates residual pigments, mainly melanins and ommochromes, which are the principal pigments responsible for colouration in insects, including BSF [20, 21, 22]. Although NaOCl is effective for pigment removal, alternative oxidants such as H_2O_2 may offer a more environmentally friendly approach. Chitin yield was calculated based on the dry weight of the initial BSF pupae shell powder (Equation 1).

$$\text{Chitin yield (\%)} = \frac{\text{Weight of chitin}}{\text{Weight of dried pupal shell}} \times 100 \quad (1)$$

2.4. Deacetylation of Chitin to Chitosan

The isolated chitin (3 g) was mixed with 60 mL of 50% (w/v) NaOH solution (solid–liquid ratio 1:20) and stirred continuously using a magnetic stirrer at 80°C for 1 h. The reaction mixture was then filtered, washed repeatedly with distilled water until neutral pH, and oven-dried at 60°C to obtain chitosan powder [23]. The yield of chitosan was determined using Equation (2).

$$\text{Chitosan yield (\%)} = \frac{\text{Weight of chitosan}}{\text{Weight of chitin}} \times 100 \quad (2)$$

2.5. Determination of Degree of Deacetylation (DD)

The degree of deacetylation (DD) was analysed using Fourier Transform Infrared (FTIR) spectroscopy (Bruker Alpha II, Germany) in the wavenumber range of 4000–400 cm^{-1} with 4 cm^{-1} resolution [23]. The absorbance ratio between the amide I band (1655 cm^{-1}) and the hydroxyl band (3450 cm^{-1}) was used to estimate DD using Equation (3). Prior to FTIR analysis, all samples were dried at 60°C until constant weight to minimise moisture interference in the OH stretching region. Baseline correction was applied using the standard instrument software prior to calculating absorbance ratios.

$$\text{DD (\%)} = \left[1 - \frac{A_{1655}/A_{3450}}{1.33}\right] \times 100 \quad (3)$$

2.6. Characterization of Chitin and Chitosan

2.6.1. Determination of the Water and Ash Content

Moisture content determination followed the AOAC method [24]. An empty weighing dish was first dried in an oven at 105°C for 1 h, cooled in a desiccator for 15 mins, and weighed. Approximately 1 g of chitin/chitosan sample was then placed in the dish and dried at 105°C for 2 h. After cooling in a desiccator for 30 mins, the dish containing the dried sample was reweighed. The drying and weighing steps were repeated until a constant weight was obtained. The moisture content (%) was calculated using Equation (4).

$$\text{Moisture content (\%)} = \frac{\text{Weight of dried sample}}{\text{Weight of initial sample}} \times 100\% \quad (4)$$

Ash content determination followed the AOAC procedure [25]. A porcelain crucible was dried in an oven at 105°C for 1 h, cooled in a desiccator for 15 mins, and weighed. Approximately 1 g of the chitosan sample was placed in the crucible and preheated over a Bunsen burner until no smoke was observed. The crucible was then transferred to a muffle furnace at 550–600°C for 3 h. After ashing, it was cooled in air for 15–30 min, then placed in a desiccator for 30 min, and reweighed. The process was repeated until a constant weight was obtained. The ash content (%) was calculated using Equation (5).

$$\text{Ash content (\%)} = \frac{\text{Weight of ash}}{\text{Weight of sample}} \times 100 \quad (5)$$

2.6.2. Fourier Transform Infrared Spectroscopy (FTIR)

FTIR spectra were recorded to identify functional groups and confirm the conversion of chitin to chitosan. The samples were analysed using the KBr pellet method in transmittance mode. Characteristic bands corresponding to amide, amine, and hydroxyl groups were used for qualitative confirmation.

2.6.3. X-ray Diffraction (XRD)

Crystallinity of the chitosan sample was determined using an X-ray diffractometer (Rigaku Miniflex 600) operating at 40 kV and 30 mA with CuKα radiation (λ = 0.1546 nm). The diffraction patterns were recorded over a 2θ range of 5–90° [23]. It should be noted that the Segal method provides only an approximate estimation of crystallinity and may overestimate values compared with whole-pattern fitting methods. The crystallinity index (CrI) was calculated using Equation (6).

$$\text{CrI (\%)} = \frac{I_{110} - I_{am}}{I_{110}} \times 100 \quad (6)$$

Where, I_{110} is the intensity of the crystalline peak at 2θ ≈ 20°, and I_{am} is the intensity of the amorphous region at 2θ ≈ 16°.

3. Results and Discussion

3.1. Optimization of Chitin Isolation from BSF Pupal Shells

The optimisation process using the Box–Behnken design (BBD) was successfully applied to identify the optimal parameters of acid–base concentration, immersion time, and temperature during demineralisation and deproteinization. The response variable was the chitin yield (%). The three-dimensional response surface (Figure 1A) and contour plots (Figure 1B) indicated that the interaction between HCl and NaOH concentrations significantly influenced the chitin yield.

The response surface (Figure 1A) and contour plot (Figure 1B) illustrate that HCl and NaOH concentrations interact strongly in determining chitin yield. Yield increased with higher acid strength (1–3 M HCl) as mineral dissolution improved, while excessive base concentration (> 2 M) slightly reduced yield due to partial depolymerisation. At moderate temperatures (25–30°C), deproteinization was efficient and polymer integrity was preserved, but prolonged or elevated temperatures (>50°C) decreased yield, consistent with previous studies [26, 27]. The optimal condition (3 M HCl, 1 M NaOH, 25°C, 1 h) yielded 50.83%, reflecting a balance between effective mineral/protein removal and minimal chitin degradation. Effervescence observed during demineralisation confirmed CO_2 evolution from $CaCO_3$, and the resulting brownish-white product indicated successful pigment and protein removal, supporting the good purity of the isolated chitin.

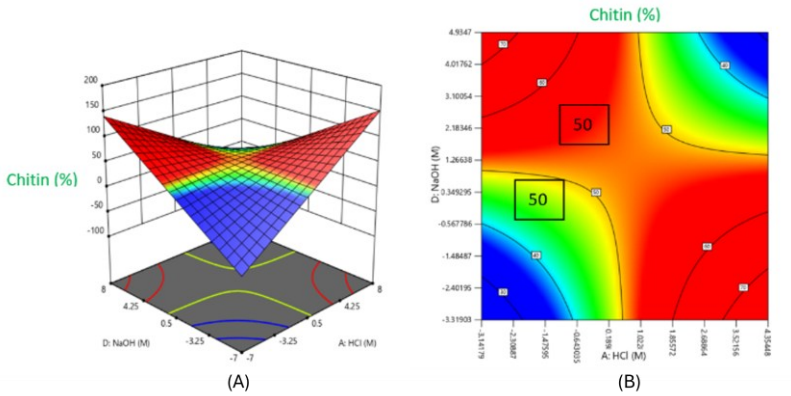

Figure 1. Response surface (A) and contour plots (B) for the effect of HCl and NaOH concentration on chitin yield

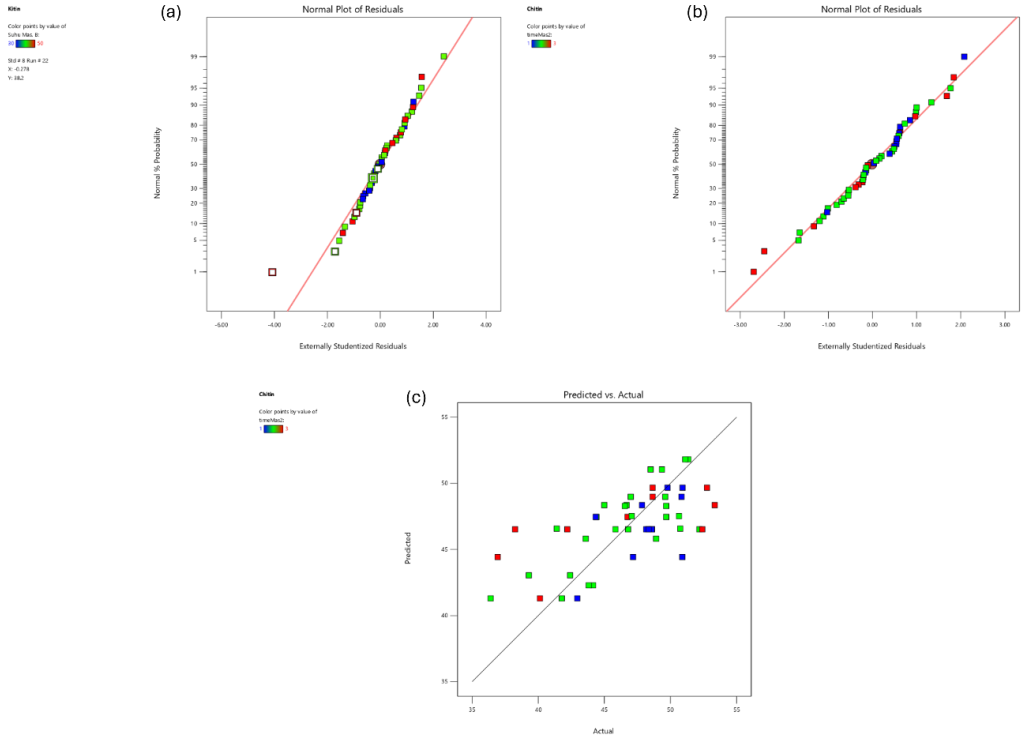

Figure 2. Diagnostic plots for the Box–Behnken regression model: (a) normal probability plot of externally studentized residuals for the initial model, (b) normal probability plot of externally studentized residuals for the refined model, and (c) predicted versus observed response plot demonstrating improved model adequacy after refinement

The optimisation model recommended by Design Expert 13 showed the highest desirability at 3 M HCl, 1 M NaOH, and 25°C for 1 h each step, predicting a chitin yield of 52.12%. Experimental validation under the same conditions produced 50.83%, confirming good agreement between predicted and experimental values (difference < 2.5%). The ANOVA analysis (Table 2) confirms that the quadratic model is statistically significant (p < 0.0001). Among the factors, HCl concentration (A), NaOH concentration (D), and NaOH soaking temperature (F) exerted the strongest effects (all p < 0.05), with a significant A×D interaction (p = 0.0465). The lack-of-fit term was not significant (p = 0.6487), indicating that the residual variation arises mainly from experimental error rather than model misspecification.

The reported R^2 value of 0.4086 indicates moderate explanatory capability, suggesting that additional factors beyond those investigated may influence chitin yield. Therefore, the model is primarily useful for identifying trends and local optimal conditions within the tested experimental range. Further studies incorporating additional variables may improve predictive accuracy. Factors with p-values greater than 0.1 were considered statistically insignificant and excluded during model refinement to improve model simplicity and interpretability. Consequently, only significant factors (A, D, F) and their interaction (AD) were retained in the final quadratic model. Diagnostic plots, including normal probability plots of residuals before and after model refinement, and a predicted-versus-observed response plot, were examined to assess model adequacy (Figure 2).

To contextualise these findings, Table 3 summarises the extraction conditions and reported chitin yields from various studies on *Hermetia illucens* (BSF) at different developmental stages. Reported chitin yields vary widely, ranging from 3.8% to 46%, depending on the concentration of acid and base, temperature, and extraction time.

Table 2. Analysis of variance (ANOVA) for the refined quadratic model

Source	Sum of Squares	df	Mean Square	F-value	p-value
Model	364.54	4	91.13	8.30	< 0.0001
A – [HCl]	45.78	1	45.78	4.17	0.0470
D – [NaOH]	110.24	1	110.24	10.04	0.0027
F – NaOH soaking temperature	162.50	1	162.50	14.80	0.0004
AD	46.02	1	46.02	4.19	0.0465
Residual (Error)	493.96	45	10.98	-	-
Lack of fit	470.50	43	10.94	0.93	0.6487
Pure error	23.46	2	11.73	-	-
Corrected total	858.50	49	-	-	-

Table 3. Extraction conditions and chitin yields from different BSF sources in previous studies

BSF Source	Demineralization			Deproteinization			Chitin Yield (%)	Reference
	Reagent (conc.)	Temp. (°C)	Time (h)	Reagent (conc.)	Temp. (°C)	Time (h)		
Larval shell	0.5 M HCOOH	RT	1	2 M NaOH	80	2	31–35	[9]
Pupal shell	1 M HCl	RT	1	1 M NaOH	80	1	30	[26]
Pupal shell	3 M HCl	RT	36	2 M NaOH	RT	36	11.8	[27]
Pupal shell	1 M HCl	RT	1	1 M NaOH	80	1	21.8–31.4	[28]
Prepupal shell	1 M HCl	RT	1	1 M NaOH	80	1	9.1–11.6	[28]
Pupal shell	1 M HCl	RT	1	1 M NaOH	80	1	9.6–11.0	[28]
Larva	0.5 M HCl	RT	2	1.9 M NaOH	50	2	46	[17]
Larva, prepupa, pupa	1 M HCl	100	0.5	1 M NaOH	80	24	3.8–6.3	[29]

Note: Differences in chitin yield arise from variations in BSF developmental stage and extraction conditions (acid/base concentration, temperature, duration). RT = room temperature.

Compared with previous reports, the optimised chitin yield obtained in this study (50.83%) is moderate yet consistent with the broad range of values reported for BSF pupae shells, which vary between 3.1 to 96.3% and 3 to 81% for chitin and chitosan, respectively [30]. The ash content of isolated chitin was 1.21%, which is comparable to values reported for purified insect-derived chitin, confirming effective mineral removal and supporting the purity of the extracted chitin. The yields of chitin and chitosan from insects are influenced by multiple factors, including species, developmental stage, rearing media, and extraction parameters. In *Hermetia illucens*, chitin content varies across developmental stages, from 3.0% in late larvae to 18.8% in pupae exuviae and 11.8% in adults, reflecting biological variability. Process conditions such as extraction time, temperature, solvent concentration, and solid–liquid ratio also play crucial roles in determining recovery efficiency. Therefore, identifying alternative chitin sources and optimising extraction parameters are essential for improving yield and achieving cost-effective industrial-scale production.

This improvement highlights the advantage of using RSM in capturing multi-factor interactions that are often overlooked by conventional one-factor-at-a-time approaches. The optimal combination of high acid concentration (3 M HCl) and mild base conditions (1 M NaOH, 25°C) enabled efficient removal of minerals and proteins without causing polymer degradation. Consequently, the developed model provides a systematic framework for identifying key process parameters influencing chitin extraction and enables the determination of locally optimal conditions, yielding results comparable to previously reported insect-derived chitin, such as beetles (20%) and desert locusts (12%) [6, 15]. Moreover, the optimised chitin yield obtained in this study (50.83%) was comparable to or even higher than those typically reported for shrimp and crab shells, which range between 19.36% and 26.08% depending on species and processing conditions [31]. This finding underscores the competitive and sustainable potential of BSF pupal shells as a non-crustacean source of chitin for future industrial applications.

3.2. Metal and Amino Acid Profiles in Demineralization and Deproteinization Filtrates

The chemical composition of the filtrates obtained during demineralisation and deproteinization of BSF pupae shells provides insight into the removal efficiency of inorganic and organic constituents. The quantitative data for metal elements and amino acids detected in the filtrates are shown in Tables 4 and 5, respectively.

Table 4. Metal content in the demineralization filtrate of BSF pupal shells

Element	Concentration (µg/g)	Fraction (%)
Ca	7,218.50	7.22×10^{-1}
Cu	1.85	1.90×10^{-4}
Fe	34.79	3.48×10^{-3}
K	3,256.98	3.26×10^{-1}
Mg	4,621.50	4.62×10^{-1}
Mn	1,133.86	1.13×10^{-1}
Na	201.73	2.01×10^{-2}
P	1,017.48	1.02×10^{-1}
Zn	30.69	3.07×10^{-3}
Total	17,517.38	1.75

Table 5. Amino-acid profile in the deproteinisation filtrate of BSF pupal shells

Amino acid	Concentration (mg/kg)	Fraction (%)
Aspartic acid	38.28	3.83×10^{-3}
Threonine	12.96	1.30×10^{-3}
Serine	26.88	2.69×10^{-3}
Glutamic acid	55.45	5.55×10^{-3}
Proline	24.15	2.42×10^{-3}
Glycine	36.11	3.61×10^{-3}
Alanine	31.13	3.11×10^{-3}
Cysteine	17.41	1.74×10^{-3}
Valine	30.78	3.08×10^{-3}
Methionine	17.01	1.70×10^{-3}
Isoleucine	11.22	1.12×10^{-3}
Leucine	26.32	2.63×10^{-3}
Tyrosine	36.12	3.61×10^{-3}
Phenylalanine	33.70	3.37×10^{-3}
Histidine	223.79	22.38×10^{-3}
Lysine	79.80	7.98×10^{-3}
Arginine	326.29	32.63×10^{-3}
Total	1027.40	102.74×10^{-3}

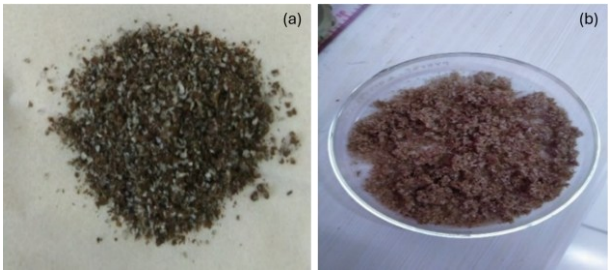

Figure 3. Physical appearance of chitin and chitosan products

Chitin, together with various proteins and calcium carbonate, is attached to the protein to form a complex network system. Demineralization refers to the removal of mineral components, mainly calcium carbonate and phosphate minerals, from organic matter by releasing CO_2 from the chitin–mineral complex. During the demineralization stage, the acid treatment with 3 M HCl dissolved most mineral salts, particularly calcium carbonate ($CaCO_3$) and calcium phosphate ($Ca_3(PO_4)_2$), resulting in effervescence caused by CO_2 evolution. The filtrate analysis showed calcium (Ca) as the predominant metal at 0.72 %, followed by magnesium (Mg, 0.46 %), potassium (K, 0.33 %), and phosphorus (P, 0.10 %).

The dominance of calcium is consistent with the known composition of insect exoskeletons, where $CaCO_3$ acts as the primary structural mineral [8, 9]. The presence of residual magnesium and potassium indicates their role as cofactors in enzymatic proteins and the natural ionic components of the insect cuticle matrix. The relatively low concentrations of these metals in the filtrate demonstrate that the acid demineralization step was effective in removing inorganic impurities from the pupal shell matrix. These results are consistent with previous findings, which also identified calcium as the predominant mineral released during HCl-based demineralization of BSF pupae shells [26, 27].

Chitin is always associated with proteins, forming a chitin–protein complex. Deproteinization is the process of removing the protein associated with chitin, forming a water-soluble amino acid. Deproteinization not only removes proteins but also pigments such as carotenoids and lipids. In the deproteinization filtrate, amino acid analysis revealed arginine (0.032%) and histidine (0.022%) as the dominant amino acids, while aspartic acid (0.014%) and glutamic acid (0.010%) were present in smaller amounts. The predominance of arginine and histidine, both basic amino acids, indicates that the proteins solubilised during the NaOH treatment were rich in nitrogen-containing residues, typical of structural and enzymatic proteins.

The presence of small amounts of acidic amino acids (aspartic and glutamic acids) reflects the partial hydrolysis of protein fragments. The alkaline deproteinization can cleave peptide bonds, liberating free amino acids and short peptides into the filtrate [1], and may vary with BSF developmental stage and diet, which influence protein composition [10, 32]. The relatively low overall amino acid concentrations indicate that the protein removal was efficient, leaving the extracted chitin

matrix with minimal organic residues. These results demonstrate that the optimised combination of 3 M HCl for demineralisation and 1 M NaOH for deproteinization successfully removed both inorganic and proteinaceous materials from BSF pupae shells [26, 27]. This efficiency contributed to a high chitin yield (50.83%) and to improved chitosan purity after deacetylation.

The inclusion of a bleaching step during chitin extraction depends on the desired colour of the final product [33]. The pigmentation in insects, including BSF, mainly arises from melanins and ommochromes. Melanins in BSF are typically classified according to their water solubility and are generally identified as eumelanins or semiquinones in nature [20, 21, 22]. Ommochromes, which possess a phenoxazine-based structure, represent another major pigment group in BSF and consist of dimers and oligomers of kynurenine. These pigments not only determine the colouration of BSF but also offer promising potential as renewable pigment sources for future applications [34, 35]. Physical appearance of chitin obtained from BSF pupae shells after the demineralisation, deproteinization, and bleaching step appears as a brownish solid, while the chitosan product obtained from the deacetylation process shows a lighter brown colour (Figure 3).

The pattern of metal release confirms that Ca and Mg are the key inorganic constituents of BSF pupae shells, while the low P and K levels suggest that phosphate and salt residues were effectively removed. The efficient demineralisation is further supported by the clear colour change and CO_2 effervescence observed during acid treatment, indicating complete dissolution of carbonate minerals. The amino acid composition of the deproteinization filtrate supports the conclusion that alkaline treatment effectively solubilised protein components, as basic amino acids were predominant while acidic and neutral amino acids were present only in trace amounts. This suggests that the optimised deproteinization conditions (1 M NaOH, 25°C, 1 h) were sufficient to hydrolyse surface-bound proteins without degrading the polysaccharide backbone. Overall, these findings demonstrate that the optimized acid–base treatment protocol not only maximised chitin yield but also enhanced purity by minimising mineral and protein residues. The released amino acids and dissolved minerals in the filtrate further confirm that the waste generated in the process could be valorised for nutrient recovery or biofertilizer applications, supporting the concept of resource-efficient and circular bioprocessing.

3.3. Characterization of Chitin and Chitosan Derived from BSF Pupal Shells

The physicochemical characteristics of chitin and chitosan isolated from BSF pupae shells are summarized in Table 6. The optimized extraction and deacetylation processes resulted in the successful conversion of chitin to chitosan, as reflected in the yield, degree of deacetylation (DD), crystallinity index (CrI), and spectral features. The chitosan exhibited a yield of 36%, a DD of 53%, and a CrI of 57%, confirming the effective transformation of chitin into partially deacetylated chitosan with moderate crystallinity.

The optimised extraction process produced chitin from BSF pupae shells with a yield of 50.83%. This chitin was subsequently converted to chitosan by alkaline deacetylation with 50% NaOH at 80°C for 1 h. The process yielded 1.08 g of chitosan from 3.01 g of chitin, corresponding to a conversion yield of 36% relative to chitin mass. The moisture and ash contents of chitin and chitosan derived from BSF pupae shells are shown in Table 6. The moisture content complies with the national quality standard (≤12%) [36], while the ash content indicates the presence of residual inorganic components, suggesting that further purification may be required to meet stricter industrial specifications. These parameters reflect the material's purity and overall quality. Ash content indicates the proportion of inorganic residues remaining after combustion, where lower values correspond to higher chitosan purity. Excessive ash can impair chitosan's performance in biomedical or food applications. Hence, maintaining optimal moisture and minimal ash levels is essential to ensure the production of high-quality chitosan suitable for industrial, agricultural, and environmental uses.

The higher ash content observed in chitosan (7.45%) compared to chitin (1.21%) may be attributed to the formation of inorganic sodium salts during alkaline deacetylation with concentrated NaOH. Residual sodium ions may remain trapped within the polymer matrix or form stable mineral complexes that are not completely removed during washing. Additionally, partial carbonisation during high-temperature ashing may contribute to apparent ash values. Similar observations have been reported in insect-derived chitosan subjected to strong alkaline treatment.

Table 6. Physicochemical characteristics of chitin and chitosan derived from BSF pupal shells

Parameter	Chitin	Chitosan
Color	Brownish-white	Light brown
Yield (%)	50.83	36
Water content (%)	8.29	4.41
Ash content (%)	1.21	7.45
Major FTIR bands (cm^{-1})	3450 (O–H/N–H), 1667 (Amide I), 1560 (Amide II)	3450 (O–H/N–H), 1650 (Amide I), 1560 (Amide II)
Degree of deacetylation (%)	35	53
Crystallinity index (%)	—	57
Dominant peaks (2θ, °)	9.6° and 19.6°	9.4°, 19.36°, 26.21°, 39.07°
Mineral residues	$CaCO_3$ (traces)	$CaCO_3$ (traces)

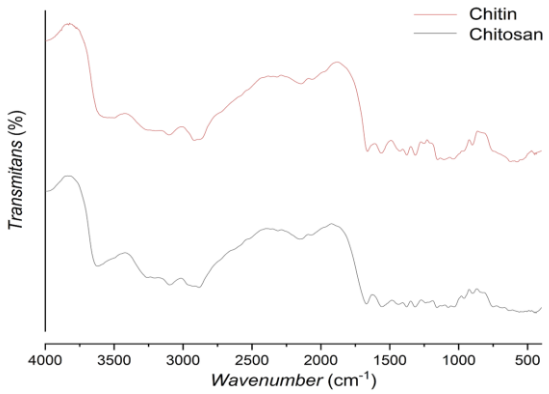

Figure 4. FTIR spectra of chitin and chitosan obtained from optimized extraction and deacetylation processes of BSF pupal shells

FTIR spectroscopy was employed to identify the molecular structure and functional groups of chitin and chitosan extracted from BSF pupae shells. The representative spectra are shown in Figure 4. The absorption band at 1615–1665 cm^{-1} corresponds to the C=O stretching of acetyl ($-COCH_3$) groups, confirming the presence of N-acetylglucosamine in chitin. In chitosan, this band appears slightly broadened and shifted toward lower wavenumbers (1635–1670 cm^{-1}), reflecting partial deacetylation and the coexistence of acetyl and amino functionalities. The amide I band (1560–1667 cm^{-1}), attributed to N–H bending vibrations, becomes more distinct as deacetylation progresses, indicating an increased proportion of glucosamine units. The presence of the amide I band at ~1560 cm^{-1} confirms partial deacetylation, consistent with the moderate DD value obtained. A broad band at 3330–3490 cm^{-1} corresponds to overlapping O–H and N–H stretching vibrations, related to intermolecular and intramolecular hydrogen bonding within the polymer matrix [30]. Overall, these changes confirm conversion of chitin to chitosan with a DD of approximately 53%, consistent with FTIR estimation.

Deacetylation in insects involves removing acetyl groups from chitin to produce chitosan, commonly using NaOH as the deacetylating agent. This process hydrolyzes N-acetylglucosamine (GlcNAc) units into glucosamine (GlcN) units, and the DD expressed as a percentage represents the proportion of GlcN units within the chitosan chain. The DD of chitosan is a critical parameter because it directly affects its physicochemical and biological properties, determining its suitability for various industrial applications.

In this study, DD values were determined by FTIR analysis, yielding 35% for chitin and 53% for chitosan (Table 6). The increase in DD confirms successful cleavage of acetamide (GlcNAc) groups and the introduction of amine (GlcN) functionalities, marking the structural conversion from chitin to chitosan. According to Kozma *et al.* [37], DD values above 50% indicate the formation of chitosan, while lower values suggest a predominance of chitin. Previous studies on Dipteran insects, such as *Hermetia illucens*, reported DD ranges of 66–93% [16, 38, 39, 40, 41]. Reaction temperature, time, particle size, and alkali concentration are key factors influencing DD [27, 42]. The moderate conditions applied in this study (80°C for 1 h) achieved sufficient deacetylation while minimising polymer degradation. Higher DD corresponds to a greater proportion of GlcN units and increased protonated amino groups, enhancing the cationic nature of chitosan. Thus, high-DD chitosan is suitable for antimicrobial, drug delivery, and wastewater treatment applications, whereas lower-DD chitosan is more suitable for biodegradable films, coatings, and controlled-release systems [30]. FTIR-based DD estimation provides a semi-quantitative approximation, and a more accurate determination may be achieved using ^1H NMR or titration methods.

XRD analysis was employed to evaluate the crystalline structures of chitin and chitosan samples. Crystallinity assessment is essential for understanding the molecular organisation of insect-derived chitin and chitosan, as it directly affects their mechanical strength, solubility, and interaction potential. The XRD pattern of BSF-derived chitosan (Figure 5) displayed distinct diffraction peaks at 2θ = 9.35° and 19.73°, corresponding to the (020) and (110) planes of chitosan (JCPDS #39-1894) [23]. Additional minor reflections observed at 26.27°, 29.41°, and 39.09° were attributed to $CaCO_3$ residues (JCPDS #47-1743), indicating the presence of trace mineral impurities [23, 43].

CrI of the chitosan was calculated to be 57% (Table 6), signifying a moderate level of crystallinity. Wang *et al.* [44] reported that the crystallinity of *Hermetia illucens* chitin varies considerably across developmental stages 33.09% in larvae, 35.14% in prepupae, 68.44% in puparia, and 87.92% in adults. Compared with crustacean-derived chitosan (70–80%), this lower CrI reflects the less ordered and more amorphous microstructure typical of insect chitin. Moderate crystallinity enhances solubility and chemical reactivity, making BSF-derived chitosan suitable for functional modification and adsorption-based applications [45]. Therefore, crystalline analysis of insect-derived chitin and chitosan is crucial for elucidating their fundamental physicochemical properties and tailoring these biopolymers to meet the requirements of future industrial and biomedical applications.

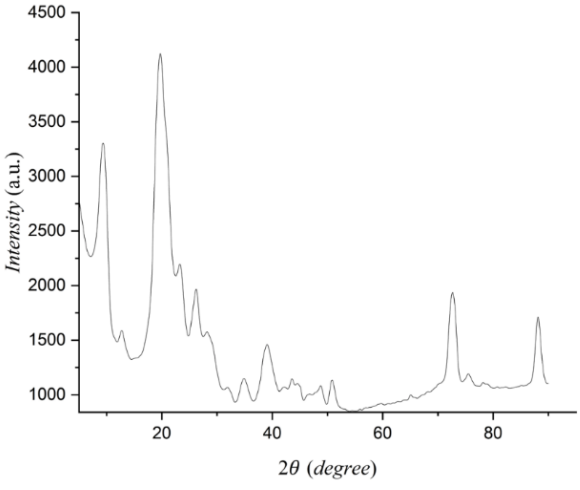

Figure 5. XRD patterns of chitosan extracted from BSF pupal shells, showing a reduction in crystallinity after deacetylation

The combined results of FTIR, XRD, and compositional analyses demonstrate that the optimised process successfully produced chitosan with a DD of 53%, CrI of 57%, and a yield of 36% from chitin with a yield of 50.83%. The material exhibited low residual mineral and protein content, confirming substantial removal of these impurities. The BSF-derived chitosan exhibited balanced physicochemical properties: sufficient rigidity from crystalline domains, yet reactive enough for chemical modification via amine groups. This semi-crystalline structure makes it suitable for use in biosorbent, bioplastic, or biomedical applications where moderate solubility and mechanical integrity are required [46]. These results highlight the potential of BSF pupal shells as a sustainable, renewable source of chitin and chitosan, providing quality comparable to that of crustacean-based materials while aligning with green chemistry and circular bioeconomy principles [47].

This study provides the first systematic optimization of chitin isolation from BSF pupae shells using a Box–Behnken design, achieving higher yields and improved process optimization compared to previous non-optimized methods. The combination of FTIR and XRD characterization confirmed the chemical integrity and structural transformation of chitin into partially deacetylated chitosan. Although the DD is lower than commercial high-grade chitosan (>70%), this level is adequate for applications such as biosorbents, biodegradable films, and controlled-release materials. The process demonstrates a sustainable and efficient valorization of BSF waste into eco-friendly biopolymers, supporting circular bioeconomy initiatives. Future optimization could include extended deacetylation or multi-step alkali treatment to achieve higher DD, as well as functional testing of the resulting chitosan for applications in biosorbent systems, biodegradable packaging, or biomedical materials.

4. Conclusion

The Box–Behnken design provided a systematic framework for identifying key process parameters influencing chitin yield and for determining locally optimal extraction conditions, achieving chitin yields of 50.83% and chitosan conversion yields of 36%. The degree of deacetylation increased from 35% to 53%, confirming the formation of partially deacetylated chitosan. FTIR and XRD analyses verified the structural transformation and moderate crystallinity (CrI = 57%). The optimized process effectively removed mineral and protein impurities, producing chitosan with moderate purity suitable for further modification. These results demonstrate that BSF pupae shells are a sustainable source of chitin and chitosan and highlight the potential of statistical optimization for future scale-up of biopolymer production. This grade of chitosan is particularly suitable for adsorption-based applications, biodegradable materials, and environmental remediation, where moderate DD and crystallinity are advantageous. Further work should focus on scaling up the optimized process and evaluating the physicochemical stability of BSF-derived chitosan for practical applications.

Acknowledgement

The authors would like to express their sincere gratitude for the financial support provided by the Riset dan Inovasi Nusantara (RiNa) Grant Program, Fiscal Year 2023–2024 (No. 481/IT3.D10/PT.01.03/P/B/2023), and for the research facilities made available by the Department of Chemistry, IPB University.

References

[1] Islem Younes, Marguerite Rinaudo, Chitin and Chitosan Preparation from Marine Sources. Structure, Properties and Applications, *Marine Drugs*, 13, 3, (2015), 1133-1174 https://doi.org/10.3390/md13031133

[2] Hanna L. Schäfer, Lars Gandras, Laura Schneider, Marco Witthohn, Kerstin Troidl, Kai Muffler, Clemens K. Weiss, Analysis, Properties, and Applications of Insect-Derived Chitosan: A Sustainable Path to Functional Polysaccharide Materials, *Gels*, 11, 4, (2025), 291-317 https://doi.org/10.3390/gels11040291

[3] V. V. Arya Lakshmi, R. Jayakumar, Chitosan: The Versatile Biomaterial, in: R. Jayakumar (Ed.) *Chitosan for Biomaterials V: Insight into Pharmaceutical Uses*, Springer Cham, Switzerland, 2024, https://doi.org/10.1007/12_2024_181

[4] Saeid Mezail Mawazi, Mohit Kumar, Noraini Ahmad, Yi Ge, Syed Mahmood, Recent Applications of Chitosan and Its Derivatives in Antibacterial, Anticancer, Wound Healing, and Tissue Engineering Fields, *Polymers (Basel)*, 16, 10, (2024), 1351-1385 https://doi.org/10.3390/polym16101351

[5] Monika Yadav, Priynshi Goswami, Kunwar Paritosh, Manish Kumar, Nidhi Pareek, Vivekanand Vivekanand, Seafood waste: a source for preparation of commercially employable chitin/chitosan materials, *Bioresources and Bioprocessing*, 6, 8, (2019), https://doi.org/10.1186/s40643-019-0243-y

[6] Murat Kaya, Talat Baran, Meltem Asan-Ozusaglam, Yavuz Selim Cakmak, Kabil Ozcan Tozak, Abbas Mol, Ayfer Mentes, Goksal Sezen, Extraction and Characterization of Chitin and Chitosan with Antimicrobial and Antioxidant Activities from Cosmopolitan Orthoptera Species (Insecta), *Biotechnology and Bioprocess Engineering*, 20, (2015), 168-179 https://doi.org/10.1007/s12257-014-0391-z

[7] Adam Waśko, Piotr Bulak, Magdalena Polak-Berecka, Katarzyna Nowak, Cezary Polakowski, Andrzej Bieganowski, The first report of the physicochemical structure of chitin isolated from *Hermetia illucens*, *International Journal of Biological Macromolecules*, 92, (2016), 316-320 https://doi.org/10.1016/j.ijbiomac.2016.07.038

[8] Mark D. Finke, Complete Nutrient Content of Four Species of Feeder Insects, *Zoo Biology*, 32, 1, (2013), 27-36 https://doi.org/10.1002/zoo.21012

[9] Thomas Hahn, Elena Tafi, Aman Paul, Rosanna Salvia, Patrizia Falabella, Susanne Zibek, Current state of chitin purification and chitosan production from insects, *Journal of Chemical Technology and Biotechnology*, 95, 11, (2020), 2775-2795 https://doi.org/10.1002/jctb.6533

[10] April Hari Wardhana, Black Soldier Fly (*Hermetia illucens*) as an Alternative Protein Source for Animal Feed, *Wartazoa*, 26, 2, (2016), 69-78

[11] Judy Retti Witono, Febianus Ferdo Setyadi, Putu Padmareka Deandra, Kevin Cleary Wanta, Arry Miryanti, Herry Santoso, Dewi Apri Astuti, Christiani Dewi Q. M. Bulin, A Comprehensive Analysis of Chitin Extraction from the Black Soldier Fly for Chitosan Production, *Periodica Polytechnica Chemical Engineering*, 68, 3, (2024), 507-522 https://doi.org/10.3311/PPch.23714

[12] Clara Pedrazzani, Lara Righi, Ferdinando Vescovi, Lara Maistrello, Augusta Caligiani, Black soldier fly as a New chitin source: Extraction, purification and molecular/structural characterization, *LWT-Food Science and Technology*, 191, (2024), 115618 https://doi.org/10.1016/j.lwt.2023.115618

[13] Anqi Xiong, Linsen Ruan, Kaiyu Ye, Zhiyong Huang, Chan Yu, Extraction of Chitin from Black Soldier Fly (*Hermetia illucens*) and Its Puparium by Using Biological Treatment, *Life*, 13, 7, (2023), 1424 https://doi.org/10.3390/life13071424

[14] M. K. Rasweefali, S. Sabu, K. S. M. Azad, M. K. R. Rahman, K. V. Sunooj, A. Sasidharan, K. K. Anoop, Influence of Deproteinization and Demineralization Process Sequences on the Physicochemical and Structural Characteristics of Chitin Isolated from Deep-sea Mud shrimp (*Solenocera hextii*), *Advances in Biomarker Sciences and Technology*, 4, (2022), 12-27 https://doi.org/10.1016/j.abst.2022.03.001

[15] Narguess H. Marei, Emtithal Abd El-Samie, Taher Salah, Gamal R. Saad, Ahmed H. M. Elwahy, Isolation and characterization of chitosan from different local insects in Egypt, *International Journal of Biological Macromolecules*, 82, (2016), 871-877 https://doi.org/10.1016/j.ijbiomac.2015.10.024

[16] Micaela Triunfo, Elena Tafi, Anna Guarnieri, Rosanna Salvia, Carmen Scieuzo, Thomas Hahn, Susanne Zibek, Alessandro Gagliardini, Luca Panariello, Maria Beatrice Coltelli, Angela De Bonis, Patrizia Falabella, Characterization of Chitin and Chitosan Derived from *Hermetia illucens*, a Further Step in a Circular Economy Process, *Scientific Reports*, 12, (2022), 6613 https://doi.org/10.1038/s41598-022-10423-5

[17] Adelya Khayrova, Sergey Lopatin, Valery Varlamov, Black Soldier Fly *Hermetia illucens* as a Novel Source of Chitin and Chitosan, *International Journal of Sciences*, 8, 4, (2019), 81-86 https://doi.org/10.18483/ijSci.2015

[18] K. M. Dimpe, J. C. Ngila, N. Mabuba, P. N. Nomngongo, Evaluation of sample preparation methods for the detection of total metal content using inductively coupled plasma optical emission spectrometry (ICP-OES) in wastewater and sludge, *Physics and Chemistry of the Earth, Parts A/B/C*, 76–78, (2015), 42-48 https://doi.org/10.1016/j.pce.2014.11.006

[19] Anne-Sofie G. Rehlund, Tessa S. Canoy, Dennis S. Nielsen, Marianne N. Lund, Mahesha M. Poojary, Protein hydrolysis for amino acid analysis revisited, *Food Chemistry*, 495, (2025), 146224 https://doi.org/10.1016/j.foodchem.2025.146224

[20] Augusta Caligiani, Angela Marseglia, Giulia Leni, Stefania Baldassarre, Lara Maistrello, Arnaldo Dossena, Stefano Sforza, Composition of black soldier fly prepupae and systematic approaches for extraction and fractionation of proteins, lipids and chitin, *Food Research International*, 105, (2018), 812-820 https://doi.org/10.1016/j.foodres.2017.12.012

[21] John E. Wertz, James R. Bolton, Biological Applications of Electron Spin Resonance, in: *Electron Spin Resonance*, Springer, Dordrecht, 1986, https://doi.org/10.1007/978-94-009-4075-8_14

[22] Nina Ushakova, Alexander Dontsov, Natalia Sakina, Alexander Bastrakov, Mikhail Ostrovsky, Antioxidative Properties of Melanins and Ommochromes from Black Soldier Fly *Hermetia illucens*, *Biomolecules*, 9, 9, (2019), 408 https://doi.org/10.3390/biom9090408

[23] F. A. Al Sagheer, M. A. Al-Sughayer, S. Muslim, M. Z. Elsabee, Extraction and characterization of chitin and chitosan from marine sources in Arabian Gulf, *Carbohydrate Polymers*, 77, 2, (2009), 410-419 https://doi.org/10.1016/j.carbpol.2009.01.032

[24] AOAC 925.10-1925, Solids (Total) and Loss on Drying (Moisture) ini Flour: Air Oven Method, in: G.W. Latimer Jr (Ed.) *Official Methods of Analysis of AOAC International*, AOAC International, Rockville, MD, 2023, https://doi.org/10.1093/9780197610145.003.2929

[25] AOAC Official Method 923.03, Ash of Flour: Direct Method, in: G.W. Latimer, Jr. (Ed.) *Official Methods of Analysis of AOAC International*, Oxford University Press, New York, 2023, https://doi.org/10.1093/9780197610145.003.2929

[26] Lilis Sulistyawati, Foliatini Foliatini, Nurdiani Nurdiani, Fitria Puspita, Isolasi dan Karakterisasi Kitin dan Kitosan dari Pupa *Black Soldier Fly* (BSF), *Jurnal WARTA AKAB*, 46, 1, (2022), 56-62 https://doi.org/10.55075/wa.v46i1.89

[27] Sri Wahyuni, Ranti Selvina, Ridha Fauziyah, Haryo Tejo Prakoso, Priyono Priyono, Siswanto, Optimasi Suhu dan Waktu Deasetilasi Kitin Berbasis Selongsong Maggot (*Hermetia ilucens*) menjadi Kitosan, *Jurnal Ilmu Pertanian Indonesia*, 25, 3, (2020), 373-381 https://doi.org/10.18343/jipi.25.3.373

[28] Lise Soetemans, Maarten Uyttebroek, Leen Bastiaens, Characteristics of chitin extracted from black soldier fly in different life stages, *International Journal of Biological Macromolecules*, 165, (2020), 3206-3214 https://doi.org/10.1016/j.ijbiomac.2020.11.041

[29] Ruben Smets, Bert Verbinnen, Ilse Van De Voorde, Guido Aerts, Johan Claes, Mik Van Der Borght, Sequential Extraction and Characterisation of Lipids, Proteins, and Chitin from Black Soldier Fly (*Hermetia illucen*) Larvae, Prepupae, and Pupae, *Waste and Biomass Valorization*, 11, (2020), 6455-6466 https://doi.org/10.1007/s12649-019-00924-2

[30] Zhenying Mei, Pavel Kuzhir, Guilhem Godeau, Update on Chitin and Chitosan from Insects: Sources, Production, Characterization, and Biomedical Applications, *Biomimetics*, 9, 5, (2024), 297 https://doi.org/10.3390/biomimetics9050297

[31] Olaosebikan Abidoye Olafadehan, Kehinde Olawale Amoo, Tolulase Olufunmilayo Ajayi, Victor Ehigimetor Bello, Extraction and Characterization of Chitin and Chitosan from *Callinectes amnicola* and

Penaeus notialis Shell Wastes, *Journal of Chemical Engineering and Materials Science*, 12, 1, (2021), 1-30 https://doi.org/10.5897/JCEMS2020.0353

[32] Chao Huang, Weiliang Feng, Jing Xiong, Teilin Wang, Weiguo Wang, Cunwen Wang, Fang Yang, Impact of Drying Method on the Nutritional Value of the Edible Insect Protein from Black Soldier Fly (*Hermetia illucens* L.) Larvae: Amino Acid Composition, Nutritional Value Evaluation, In Vitro Digestibility, and Thermal Properties, *European Food Research and Technology*, 245, 1, (2019), 11-21 https://doi.org/10.1007/s00217-018-3136-y

[33] Nurul Alyani Zainol Abidin, Faridah Kormin, Nurul Akhma Zainol Abidin, Nor Aini Fatihah Mohamed Anuar, Mohd Fadzelly Abu Bakar, The Potential of Insects as Alternative Sources of Chitin : An Overview on the Chemical Method of Extraction from Various Sources, *International Journal of Molecular Sciences*, 21, 14, (2020), 4978 https://doi.org/10.3390/ijms21144978

[34] R. K. Toner, Recent Progress in the Chemistry of Natural and Synthetic Colouring Matters and Related Fields, *Textile Research Journal*, 33, 7, (1963), 580 https://doi.org/10.1177/004051756303300710

[35] Florent Figon, Jérôme Casas, Ommochromes in Invertebrates: Biochemistry and Cell Biology, *Biological Reviews*, 94, 1, (2018), 156-183 https://doi.org/10.1111/brv.12441

[36] Badan Standar Nasional Indonesia, *Kitosan-Syarat Mutu dan Pengolahan (SNI 7949-2013)*, BSN Press, Jakarta, 2013,

[37] Michael Kozma, Bishnu Acharya, Rabin Bissessur, Chitin, Chitosan, and Nanochitin: Extraction, Synthesis, and Applications, *Polymers*, 14, 19, (2022), 3989 https://doi.org/10.3390/polym14193989

[38] A. Antonov, G. Ivanov, N. Pastukhova, G. Bovykina, Production of chitin from dead Hermetia Illucens, *IOP Conference Series: Earth and Environmental Science*, 315, (2019), 042003 https://doi.org/10.1088/1755-1315/315/4/042003

[39] Teo Hui Peng, Law Ke Wei, Eric Chan Wei Chiang, Michelle Soo Oi Yoon, Antibacterial Properties of Chitosan Isolated from the Black Soldier Fly, *Hermetia illucens*, *Sains Malaysiana*, 51, 12, (2022), 3923-3935 https://doi.org/10.17576/jsm-2022-5112-05

[40] Mevin Kiprotich Lagat, Samuel Were, Francis Ndwigah, Violah Jepkogei Kemboi, Carolyne Kipkoech, Chrysantus Mbi Tanga, Antimicrobial Activity of Chemically and Biologically Treated Chitosan Prepared from Black Soldier Fly (*Hermetia illucens*) Pupal Shell Waste, *Microorganisms*, 9, 12, (2021), 2417-2429 https://doi.org/10.3390/microorganisms9122417

[41] Adelya Khayrova, Sergey Lopatin, Balzhima Shagdarova, Olga Sinitsyna, Arkady Sinitsyn, Valery Varlamov, Evaluation of Antibacterial and Antifungal Properties of Low Molecular Weight Chitosan Extracted from *Hermetia illucens* Relative to Crab Chitosan, *Molecules*, 27, 2, (2022), 577-589 https://doi.org/10.3390/molecules27020577

[42] Etty Centaury Siregar, Suryati Suryati, Lukman Hakim, Pengaruh Suhu dan Waktu Reaksi pada Pembuatan Kitosan dari Tulang Sotong (*Sepia officinalis*), *Jurnal Teknologi Kimia Unimal*, 5, 2, (2016), 37-44 https://doi.org/10.29103/jtku.v5i2.88

[43] Zidni Azizati, Pembuatan dan Karakterisasi Kitosan Kulit Udang Galah, *Walisongo Journal of Chemistry*, 2, 1, (2019), 10-16 https://doi.org/10.21580/wjc.v3i1.3878

[44] Huarui Wang, Kashif ur Rehman, Weijian Feng, Dan Yang, Rashid ur Rehman, Minmin Cai, Jibin Zhang, Ziniu Yu, Longyu Zheng, Physicochemical structure of chitin in the developing stages of black soldier fly, *International Journal of Biological Macromolecules*, 149, (2020), 901-907 https://doi.org/10.1016/j.ijbiomac.2020.01.293

[45] Nadhrah Wivanius, Emil Budianto, Sintesis dan Karakterisasi Hidrogel Superabsorben Kitosan Poli (N-Vinilkaprolaktam) (Pnvcl) dengan Metode Full Ipn (*Interpenetrating Polymer Network*), *Pharmaceutical Sciences and Research*, 2, 3, (2015), 152-168 https://doi.org/10.7454/psr.v2i3.3483

[46] Ranjeet Desai, Radhika Pachpore, Ashwini Patil, Ratnesh Jain, Prajakta Dandekar, Review of the Structure of Chitosan in the Context of Other Sugar-Based Polymers, in: R. Jayakumar, M. Prabaharan (Eds.) *Advances in Polymer Science Chitosan for Biomaterials III*, Springer International Publishing, Switzerland, 2021, https://doi.org/10.1007/12_2021_89

[47] Kannan Mohan, Durairaj Karthick Rajan, Dharmaraj Divya, Jayakumar Rajarajeswaran, Shubing Zhang, Palanivel Sathishkumar, New insights into the organic waste-derived black soldier fly chitin and chitosan for biomedical and industrial applications, *Journal of Environmental Chemical Engineering*, 12, 6, (2024), 114660 https://doi.org/10.1016/j.jece.2024.114660